

Supporting Information

Heterojunction structured MnCO₃@NiO composites and their enhanced electrochemical performance

Zexian Zhang^a, Tao Mei^{*a}, Kai Yang^a, Jing Li^a, Zhi Tao^a, Yuting xiong^b, Liangbiao Wang^{*b}

a Hubei Collaborative Innovation Center for Advanced Organic Chemical Materials, Ministry-of-Education Key Laboratory for the Green Preparation and Application of Functional Materials, Hubei Key Laboratory of Polymer Materials, School of Materials Science and Engineering, Hubei University. Wuhan 430062, PR China. Email: meitao@hubu.edu.cn; Fax: +86 27 8866 1729; Tel: +86 27 8866 2132

b School of Chemistry and Environment Engineering, Jiangsu University of Technology, Changzhou 213001, P. R. China. Email: lbwang@jsut.edu.cn

Contents

Fig. S1. TG image of MnCO₃@NiO.

Fig. S2. XRD patterns of pristine MnCO₃ after sintering in 280 °C for 3 h.

Fig. S3. (a) SEM image of MnCO₃@NiO, (b),(c),(d) respectively represented C, Mn, Ni element, derived from (a).

Fig. S4. TEM image of MnCO₃@NiO.

Fig. S5. The CV curves at the scanning rate of 0.01 mV s⁻¹ of MnCO₃ and NiO, respectively.

Fig. S6. Nyquist plots of the AC impedance spectra for MnCO₃ and MnCO₃@NiO.

Fig. S7. The discharge capacity and the coulombic efficiency of the (a) MnCO₃ and (b) NiO at 1.0 A g⁻¹. The rate performance of (c) MnCO₃ and (d) NiO.

Fig. S8. The capacities of three samples in this work at 1.0 A g⁻¹ rate.

Fig. S9. FESEM images of MnCO₃@NiO in an electrode (a) before cycling and (b) after cycling at 1.0 A g⁻¹ over 300 cycles.

Tab. S1 The EDX results of the C, Mn and Ni element of the obtained MnCO₃@NiO

Tab. S2 Compare the obtained MnCO₃@NiO with the reported MnCO₃ and NiO as the cathode for LIBs

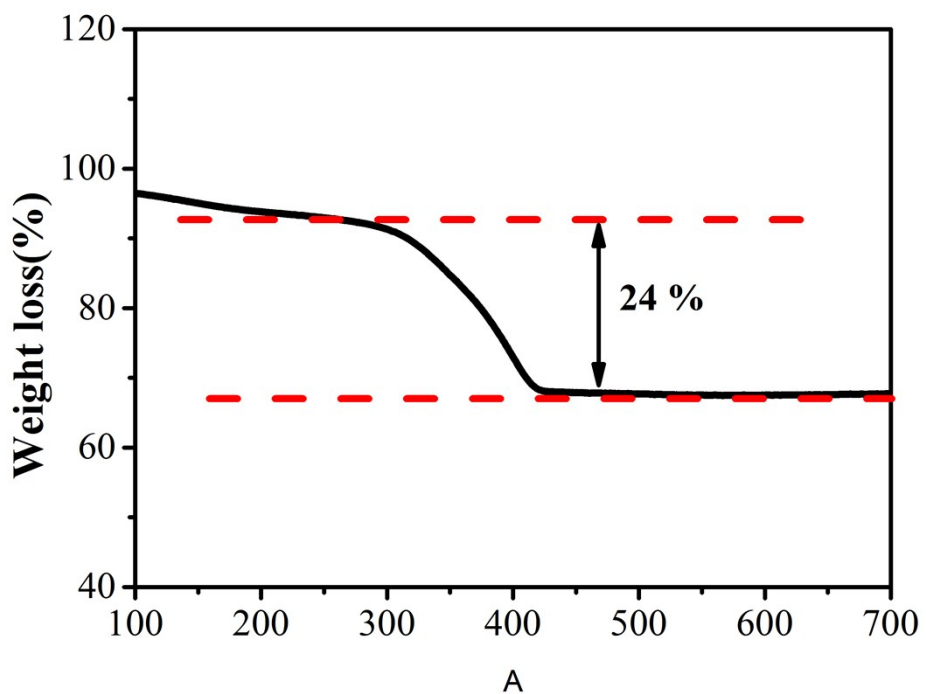


Fig. S1. TG image of $\text{MnCO}_3@\text{NiO}$.

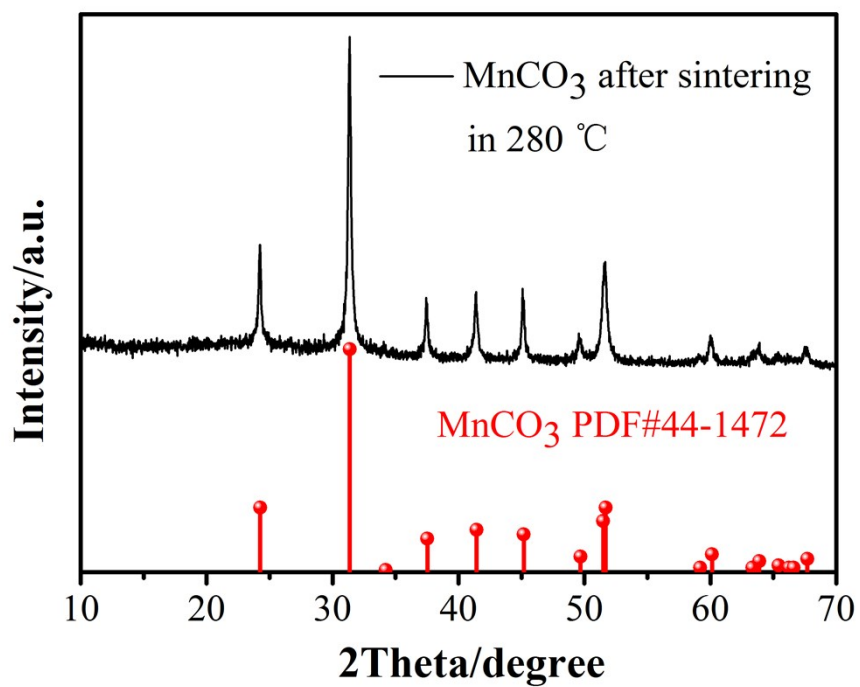


Fig. S2. XRD patterns of pristine MnCO₃ after sintering in 280 °C for 3 h.

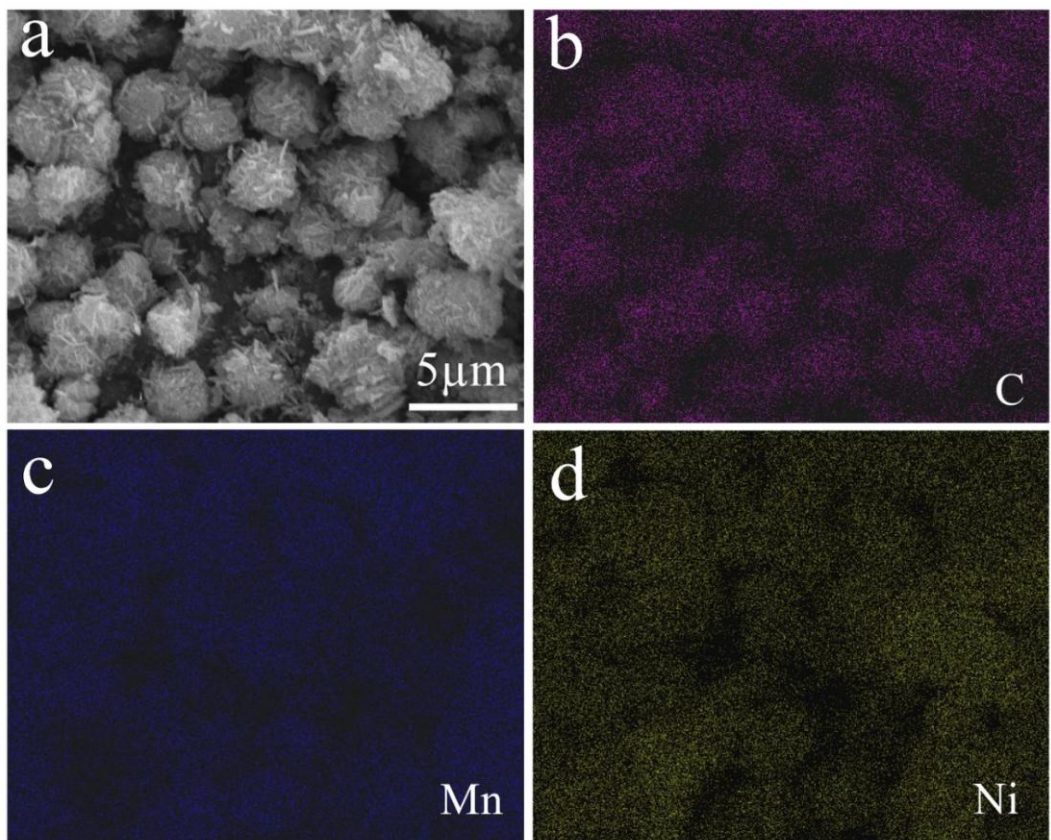


Fig. S3. (a) SEM image of $\text{MnCO}_3@\text{NiO}$, (b),(c),(d) respectively represented C, Mn, Ni element, derived from (a).

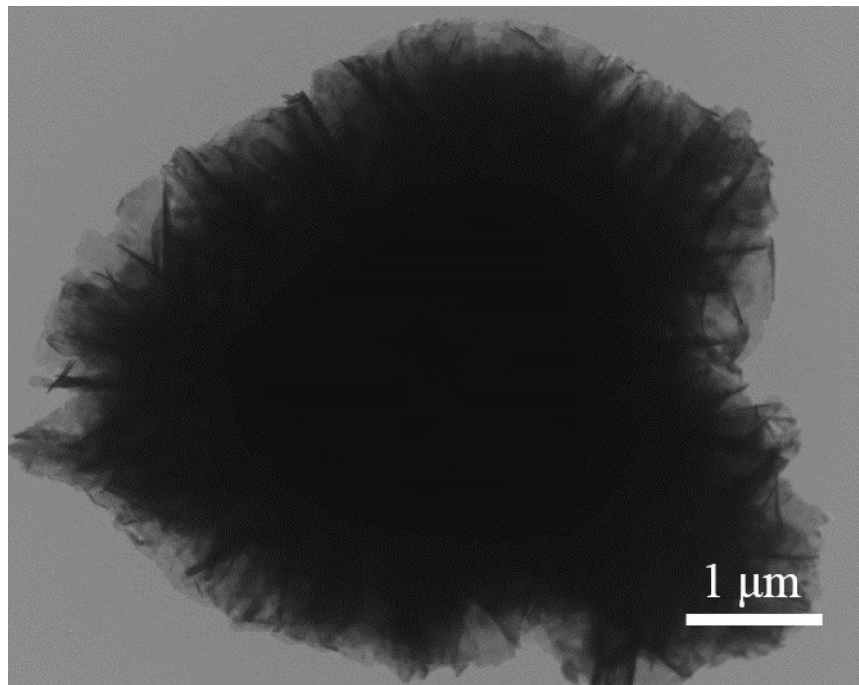


Fig. S4. TEM image of $\text{MnCO}_3@\text{NiO}$.

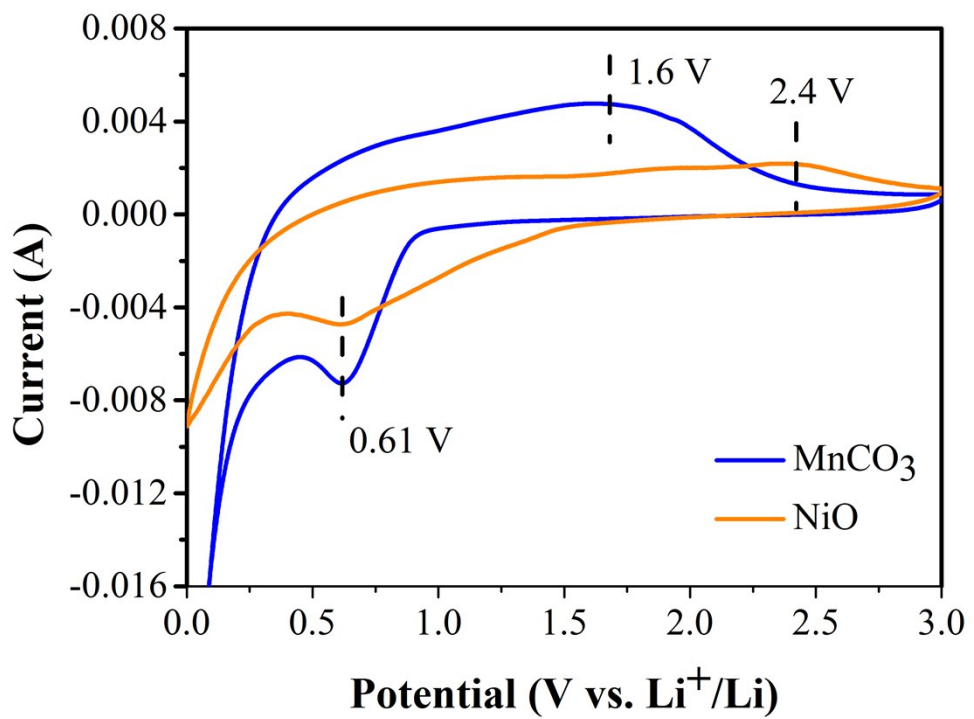


Fig. S5. The CV curves at the scanning rate of 0.01 mV s⁻¹ of MnCO₃ and NiO, respectively.

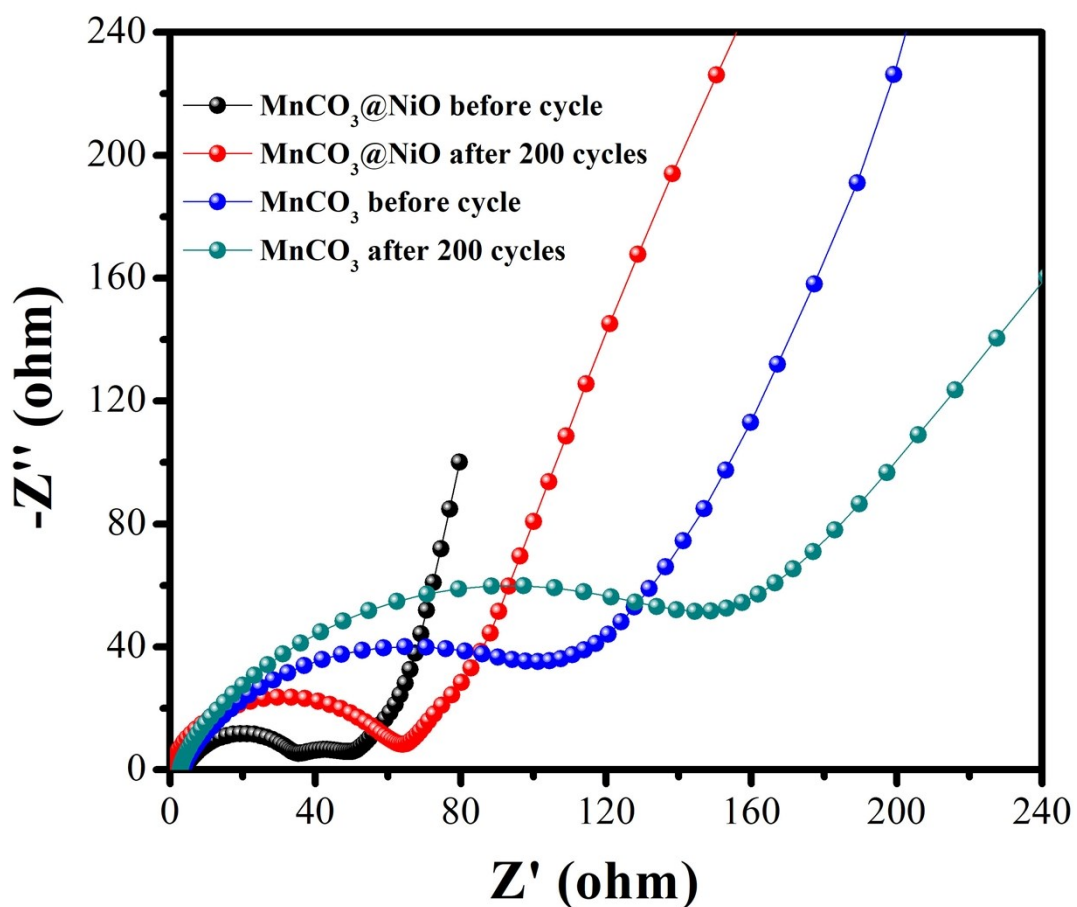


Fig. S6. Nyquist plots of the AC impedance spectra for MnCO_3 and $\text{MnCO}_3@\text{NiO}$.

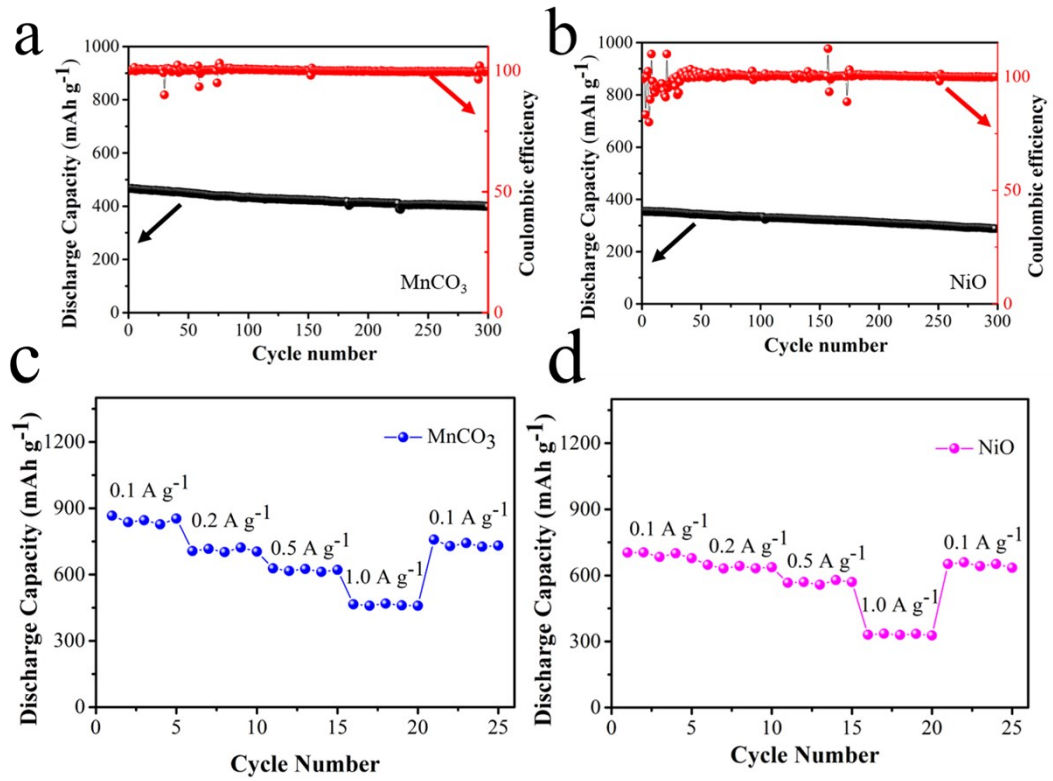


Fig. S7. The discharge capacity and the coulombic efficiency of the (a) MnCO₃ and (b) NiO at 1.0 A g⁻¹. The rate performance of (c) MnCO₃ and (d) NiO.

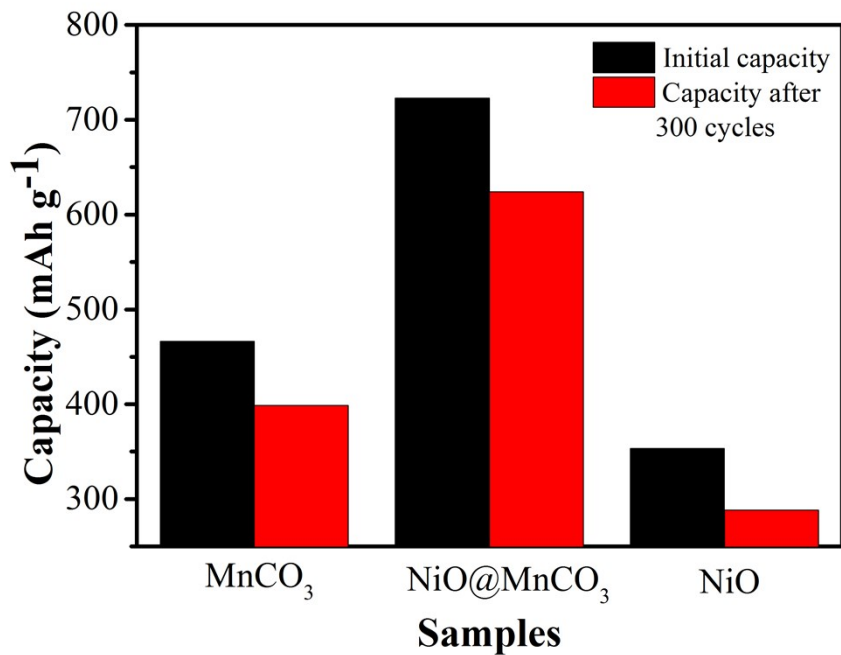


Fig. S8. The capacities of three samples in this work at 1.0 A g^{-1} rate.

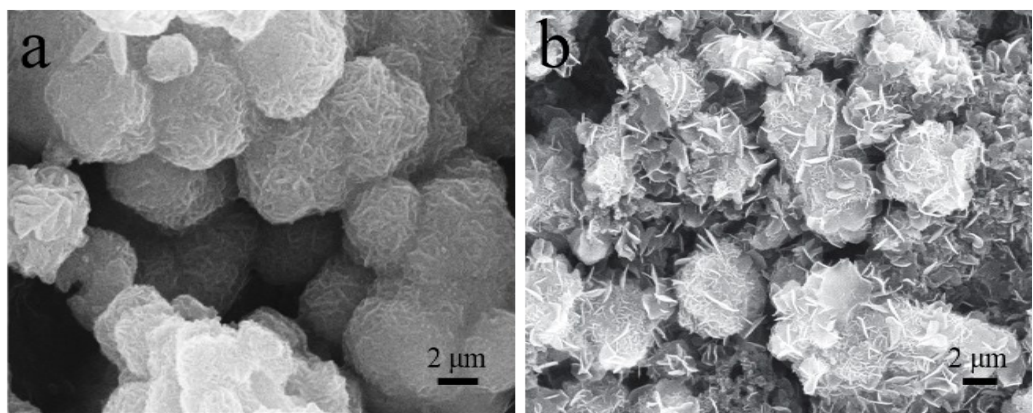


Fig.S9. FESEM images of $\text{MnCO}_3@\text{NiO}$ in an electrode (a) before cycling and (b) after cycling at 1.0 A g^{-1} over 300 cycles.

Tab. S1 The EDX results of the C,Mn and Ni element of the obtained MnCO₃@NiO.

<i>Element</i>	<i>Wt%</i>	<i>At%</i>
<i>CK</i>	10.52	36.62
<i>MnK</i>	48.29	36.66
<i>NiK</i>	41.19	12.54
<i>Matrix</i>	Correction	ZAF

Tab. S2 Compare the obtained $\text{MnCO}_3@\text{NiO}$ with the reported MnCO_3 and NiO as the anode for LIBs.

Composites	Current density (C/mA g ⁻¹)	Cycle number	Specific capacity (mAh g ⁻¹)	Ref.
MnCO_3 flower	0.2 C	200	384	1
MnCO_3 spheres	100 mA g ⁻¹	100	656	2
MnCO_3 microdumbbells	0.5 C	100	775	3
NiO nano octahedron	359 mA g ⁻¹	200	793	4
NiO nanofiber	80 mA g ⁻¹	100	784	5
NiO nanowall array	500 mA g ⁻¹	50	564	6
NiO nanowalls	0.1 C	50	844	7
NiO nanorods	100 mA g ⁻¹	60	700	8
NiO nanoflowers	0.1 C	50	552	9
NiO nanospheres	100 mA g ⁻¹	60	518	10
$\text{MnCO}_3@\text{NiO}$	100 mA g ⁻¹	300	900	Our work

References:

1. Y.L. Mu, L. Wang, Y. Zhao, M.J. Liu, W. Zhang, J.T. Wu, X. Lai, G.Y. Fan, J. Bi, D.J. Gao, *Electrochim. Acta* 251 (2017) 119-128.
2. L. Xiao, S.Y. Wang, Y.F. Wang, W. Meng, B.H. Deng, D.Y. Qu, Z.Z. Xie, J.P. Liu, *ACS Appl. Mater. Interfaces* 8 (2016) 25369-25378.
3. L. Zhang, T. Mei, X.B. Wang, J.Y. Wang, J.H. Li, W.L. Xiong, Y. Chen, M. Hao, *CrystEngComm* 17 (2015) 6450-6455.
4. C.Z. Wang, Y.J. Zhao, D.Z. Su, C.H. Ding, L. Wang, D. Yan, J.B. Li, H.B. Jin, *Electrochim. Acta* 231 (2017) 272-278.
5. V. Aravindan, P. Suresh Kumar, J. Sundaramurthy, W.C. Ling, S. Ramakrishna, S. Madhavi, *J. Power Sources* 227 (2013) 284-290.
6. F. Cao, G.X. Pan, P.S. Tang, H.F. Chen, *Mater. Res. Bull.* 48 (2013) 1178-1183.
7. Q. Wang, C.Y. Zhang, W.F. Shan, L.L. Xing, X.Y. Xue, *Mater. Lett.* 118 (2014) 66-68.
8. Q. Li, G. Huang, D.M. Yin, Y.M. Wu, L.M. Wang, *Part. Part. Syst. Char.* 33 (2016) 764-770.
9. Y.B. Mollamahale, Z. Liu, Y.D. Zhen, Z.Q. Tian, D. Hosseini, L.W. Chen, P.K. Shen, *Int. J. Hydrogen Energy* 42 (2017) 7202-7211.
10. G.H. Zhang, Y.J. Chen, B.H. Qu, L.L. Hu, L. Mei, D.N. Lei, Q. Li, L.B. Chen, Q.H. Li, T.H. Wang, *Electrochim. Acta* 80 (2012) 140-147.